Journal of Pharmaceutical and Applied Chemistry

ISSN: 2357-0210 VOLUME 3, ISSUES 1, 2017 www.egyptfuture.org/ojs/

Fragmentation Pathway of Doxazosin Drug: Thermal Analysis, Mass Spectrometry and DFT Calculations and NBO Analysis

M.El-Desawy[1], *M. A. Zayed*[2,*] *and Yasmeen Farrag*[2]

[1]Nuclear Physics Department, Nuclear Research Centre, AEA, 13759-Cairo, Egypt.
[2] Chemistry Department, Faculty of Science, Cairo University, 12613- Giza, Egypt.

Received: 5 Jul. 2016, Revised: 22 Oct. 2016, Accepted: 25 Oct. 2016.
Published online: 1 Jan. 2017.

Abstract: Doxazosin ($C_{23}H_{25}N_5O_5$) is α1-selective alpha blocker used to treat high blood pressure and urinary retention associated with benign prostatic hyperplasia (BPH). The doxazosin (DOX) drug was investigated using electron impact mass spectral (MS) fragmentation at 70 and 15 eV of electron energy, thermal analysis (TA) measurements and confirmed by molecular orbital calculations using density functional theory(DFT) calculations and natural bond orbital (NBO) analysis. The mass spectra and thermal analysis fragmentation pathways were proposed and compared to each other to select the most suitable scheme representing the correct fragmentation pathway of the drug in both techniques. The optimum molecular geometry and the total energy of the neutral and the positively charged DOX molecules were calculated by density functional theory method with 6-311G basis sets and natural bond orbitals (NBO) analysis. The molecular orbital calculations provides a base for fine distinction among sites of initial bond cleavage and subsequent fragmentation of drug molecule in both TA and MS techniques; consequently the choice of the correct pathway of such fragmentation knowing this structural session of bonds can be used to decide the active sites of this drug responsible for its chemical, biological and medical reactivity.

Keywords: Doxazosin, Mass spectrometry, Thermal analysis, Molecular Orbital Calculation, DFT, NBO

1 Introduction

Mass Spectrometry (MS) is an invaluable analytical tool which can provides a large amount of structural information with little expenditure of sample. It can also shed light on various physical characteristics such as binding energies and proton affinity within a molecule [1]. Mass spectrometry has been applied to numerous fields and areas of interest including, for example, the analysis of peptides, proteins, and nucleic acids along with applications in medical research and environmental sciences.

Thermal analytical techniques can provide important information regarding storage and stability of pharmaceuticals [2-6]. These are precise and accurate techniques with low sample requirements, and can provide detailed information about new chemical entities even at the very earliest stages of discovery and development of the new compositions and drugs [7-10]. In thermal analysis, the molecules are continuously energized and deactivated by gas evolution, where any change in energy is reflected in the change in temperature [11].

On the other hand, computational quantum chemistry can provide additional information, which can be used successfully for the interpretation of experimental results [12]. It may also be used in the description and prediction of primary fragmentation processes and subsequent one.

Through the analysis of gas phase rearrangements within the mass spectrometer and a careful comparison with thermal analysis, fragmentation and decomposition pathways can be explored. The complementary nature of these techniques has been demonstrated for some species where the fragmentation and/or subsequent degradation processes began at a similar location within the molecule, i.e.: the weaker bonds. Mass spectrometry and thermal analysis data has been useful in elucidating some structure components of newly synthesized molecules, but a universal comparison has not been possible [13]. Mass spectrometry and thermal Analysis have been around for some time, but recently there have been many studies published on MS and TA coupled with other physico-chemical methods.

Doxazosin ($C_{23}H_{25}N_5O_5$) is a selective a1-adrenergic receptor antagonist used to treat hypertension and benign prostatic hyperplasia [14–18]. The geometrical structure of Doxazosin is shown in Fig.1. Doxazosin is extensively metabolized in the liver via O-demethylation and

hydroxylation, which is <5% of the administered dose excreted unchanged in feces [19]. Determination of doxazosin in pharmaceutical formulations and biological matrices was performed using HPLC-UV [20], HPLC-FLR [21–27] and LC–MS. A method for simultaneous determination of both mass spectrometry and thermal analysis with theoretical molecular orbital calculations for doxazosin drug was not published so far [28–30]. Doxazosin was also, analyzed using electrochemical techniques [31, 32].

The aim of the present work is to propose fragmentation pathway of doxazosin drug. This work includes a correlation between, mass spectral fragmentation and thermal analysis degradation of the drug and comparing these experimental data with the density functional theory (DFT) calculation and Nature bond orbital (NBO) analysis. This comparison is used to identify the weakest bonds ruptured during both mass and thermal studies. Consequently the choice of the correct pathway of such fragmentation knowing this structural session of bonds can be used to decide the active sites of this drug responsible for its chemical, biological and medical reactivity.

2 Experimental

2.1 Mass spectrometry (MS)

Electron ionization (EI) mass spectra of DOX were obtained using Thermo Finnegan TRACE DSQ quadrupol mass spectrometer with electron multiplier detector equipped with a GC–MS data system at Atomic and Molecular physics Unit- Nuclear research Centre. The direct probe for solid material was used in this study. EI mass spectra were obtained at ionizing energy values of 70 and 15 eV, the vacuum is better than 10^{-6}torr.

2.2 Thermal analyses (TA)

The thermal analyses (TGA, DTG and DTA) were carried out in dynamic nitrogen atmosphere (20 mL min^{-1}) with a heating rate of 10 °C min^{-1} using Shimadzu system of DTG-60H thermal analyzers at Microanalytical Center Cairo University. The mass losses of 5 mg sample and heat response of the changes in the sample were measured from room temperature up to 600 ◦C. The heating rate was 10ºC min^{-1} in an inert argon atmosphere. These instruments were calibrated using indium metal as thermally stable material. The reproducibility of the instrument readings was determined by repeating each experiment more than twice.

2.3 Computational calculations

The molecular structure of the title compound in the ground state was optimized by a DFT method using B3LYP functional [33-34] combined with 6-311G basis set. Calculations were carried out using GAUSSIAN 09 [35] suite of programs. Natural bond orbitals (NBO) analysis was performed using NBO 3.1 program [36] at the same level of theory.

3 Results and Discussion

3.1 DFT Studies

3.1.1 Geometry optimization

The fully optimized geometries of DOX and numbering of atoms are shown in Fig.1. Table 1 presents the optimized structure parameter of DOX as calculated by DFT/B3LYP level of theory with 6-31G (d) basis set.

Table 1: Comparison between computed bond length (Å), bond angle (º) and Mulliken charge (e) for neutral and molecular cation of doxazosin drug.

Bond Length (Å)			Bond Angle (°)			Mulliken Charge(e)		
	Neutral	cation		Neutral	cation		neutral	cation
O1-C2	1.258	1.251	O1C2N3	122.529	119.166	O1	-0.438	-0.394
C2-N3	1.363	1.379	C2N3C4	119.205	121.242	**C2**	**0.611**	**0.549**
C2-C24	1.526	1.521	N3C4C5	110.447	119.248	N3	-0.566	-0.553
N3-C4	1.478	1.470	C4C5N6	110.146	119.406	C4	-0.183	-0.208
N3-C23	1.476	1.468	C5N6C7	117.647	117.248	C5	-0.159	-0.184
C4-C5	1.532	1.543	C7N8C9	128.972	128.910	N6	-0.602	-0.528
C5-N6	1.466	1.475	C7N21C20	124.563	121.289	C7	0.575	0.580
N6-C7	1.377	1.362	N7C8C10	113.018	112.950	N8	-0.460	-0.438
N6-C22	1.465	1.476	C8C10C11	120.355	119.834	C9	0.533	0.585
C7-N8	1.374	1.364	C10C11C12	124.397	124.085	N10	-0.839	-0.812
C7-N21	1.340	1.363	C11C12O13	124.045	115.017	C11	-0.070	-0.050
N8-C9	1.336	1.337	C11C12O14	113.560	112.871	C12	-0.068	-0.072
C9-N10	1.365	1.350	C6C1O15	115.969	115.286	C13	0.218	0.256
C9-C11	1.439	1.454	C1O15C16	118.208	121.685	O14	-0.531	-0.503
C11-C12	1.418	1.396				C15	-0.289	-0.300
C11-C20	1.423	1.440				C16	0.266	0.300
C12-C13	1.380	1.400				O17	-0.526	-0.512
C13-O14	1.396	1.364				C18	-0.284	-0.261
C13-C16	1.429	1.439				C19	-0.160	-0.133
O14-C15	1.450	1.467				C20	0.106	0.104
C16-O17	1.391	1.366				N21	-0.446	-0.397
C16-C19	1.376	1.378				C22	-0.161	-0.186
O17-C18	1.468	1.476				C23	-0.158	-0.177
C19-C20	1.416	1.417				C24	-0.183	-0.150
C20-C21	1.374	1.356				O25	-0.529	-0.560
C22-C23	1.534	1.544				C26	0.231	0.251
C24-O25	1.475	1.471				C27	-0.148	-0.142
C24-C33	1.523	1.530				C28	-0.144	-0.142
O25-C26	1.410	1.414				C29	-0.138	-0.127
C26-C27	1.393	1.392				C30	-0.156	-0.147
C26-C31	1.400	1.401				C31	0.239	0.238
C27-C28	1.396	1.395				O32	-0.511	-0.494
C28-C29	1.400	1.403				C33	-0.089	-0.070

The global minimum energy obtained by the DFT structure optimization based on B3LYP with 6-311G basis set for neutral and positively charged DOX molecule is -

1541.2838 and -1541.0387 a.u., respectively. Consequently, the neutral DOX molecule is more stable than the positively charged one because it has lower total energy.

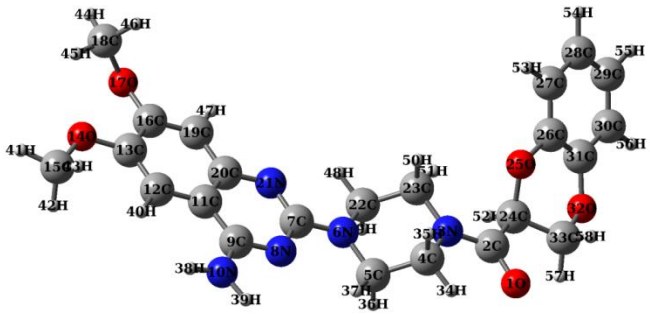

Fig. 1: The geometrical structure of Doxazosin.

When comparing among the bond length, in Table 1 for the neutral and positively charged drug, one can conclude small differences in bond length in DOX system upon ionization, indicating that no appreciable change in the geometries upon ionization.

The calculation of effective Mulliken atomic charge plays an important role in the application of quantum mechanical calculations to the molecular systems. As shown in Fig. 2. It is worthy to mention that C2 atom (0.611e), C7 atom (0.575e) and C9 atom (0.533e) possess the maximum positive charge among all carbon atoms in DOX. This is due the withdrawing effect of O, N on these atoms. It is confirmed by low charge density on C24 atom (-0.138e), C4 atom (-0.138e) and C23atom (-0.158e). Likewise, both C13 (0.218e) and C16 (0.288e) atoms have larger positive charges than the other aromatic carbons. This is due to the attachment of negatively charged O14 and O17. It can be seen that the similar atoms in cation molecule has nearly the same charge and sign as shown in Fig. 2.

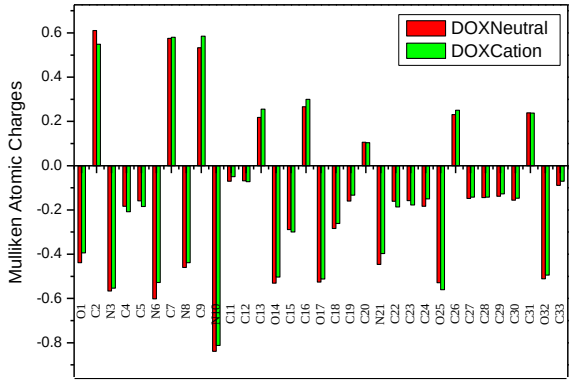

Fig. 2: Mulliken charges of neutral and cation DOX calculated at DFT/B3LYP/6-311G level of theory.

3.1.2 Natural bond orbital (NBO) analysis

The natural bond orbital (NBO) calculation was performed using NBO 3.1 program implemented in the Gaussian 09 package at the DFT/B3LYP/6-311G level in order to understand intra- and inter-molecular bonding and interaction among bonds, which is a measure of the delocalization or Hyperconjugation. The Hyperconjugative interaction energy was deduced from the second-order perturbation approach [34].

Delocalization of electron density between occupied Lewis-type (bond or lone pair) NBO orbitals and formally unoccupied (anti bond or Rydberg) non-Lewis NBO orbitals corresponds to a stabilizing donor–acceptor interaction. In NBO analysis, the larger the E(2), the more intensive is the interaction between electron donors and electron acceptors, i.e., the more donating tendency from electron donors to electron acceptors and the greater the extent of conjugation of the whole system.

The possible intensive interactions are given in Tables 2 for the neutral and positively charged DOX molecules, respectively. Delocalization of electrons of the neutral DOX is higher than that of the positively charger DOX and this results in increase in the stability of the neutral DOX in comparing to the $[DOX]^+$. For example, as shown in Table 3, π(C7–N21) → π*(C11–C20), π(N8–C9) → π*(C7–N21), π(C11–C20)→ π*(N8–C9), π(C11–C20) → π*(C12–C13) and π(C16–19) → π*(C11–C20), interactions are seen for DOX to give strong stabilization of 24.94, 30.60, 33.39, 21.11 and 18.98 kcal mol-1, respectively. Also, as presented in Table 3, π(C11–C12) → π*(C20–C21), π (C16–C19) → π *(C20–C21), π (C20–C21) → π *(C7–C8) interactions are seen for $[DOX]^+$ to give a lower stabilization of 13.99, 16.00, and 20.34 kcal mol-1, respectively.

Table 2: Second order perturbation theory analysis of Fock matrix in NBO basis of neutral DOX molecule (selected).

Donor NBO(i)	Acceptor NBO(j)	E^2 (kcal/mol)	ΔE a.u.	F(i,j) a.u.
BD (2) C7 - N21	BD*(2) C11 - C20	24.94	0.32	0.085
BD (2) N8 - C9	BD*(2) C7 - N21	30.60	0.31	0.093
BD (2) C11 - C20	BD*(2) C7 - N21	10.02	0.25	0.045
BD (2) C11 - C20	BD*(2) N8 - C9	33.39	0.24	0.080
BD (2) C11 - C20	BD*(2) C12 - C13	21.11	0.26	0.068
BD (2) C11 - C20	BD*(2) C16 - C19	14.76	0.28	0.059
BD (2) C12 - C13	BD*(2) C11 - C20	14.44	0.30	0.063
BD (2) C12 - C13	BD*(2) C16 - C19	15.89	0.31	0.063
BD (2) C16 - C19	BD*(2) C11 - C20	18.98	0.29	0.070
BD (2) C16 - C19	BD*(2) C12 - C13	18.01	0.28	0.064
BD (2) C26 - C31	BD*(2) C27 - C28	19.64	0.30	0.069
BD (2) C26 - C31	BD*(2) C29 - C30	19.03	0.30	0.068
BD (2) C27 - C28	BD*(2) C26 - C31	21.07	0.26	0.069
BD (2) C27 - C28	BD*(2) C29 - C30	19.91	0.28	0.067
BD (2) C29 - C30	BD*(2) C26 - C31	21.45	0.26	0.069
BD (2) C29 - C30	BD*(2) C27 - C28	19.94	0.28	0.067
LP (1) O1	RY*(1) C2	13.41	1.51	0.127
LP (2) O1	BD*(1) C2 - N3	20.80	0.70	0.109
LP (2) O1	BD*(1) C2 - C24	18.36	0.60	0.095

E^2 means energy of Hyperconjugative interactions

ΔE = Ej – E_i is the energy difference between donor (i) and acceptor (j) NBO orbitals; F = F(i, j) is the Fock matrix element between i and j NBO orbitals

However, the strong stabilization denotes the larger delocalization in the neutral DOX compared to that of $[DOX]^+$ molecule. However, the most important interactions of DOX molecule having lone pair LP (2) O1

with that of antibonding BD*(1) C2–N3 and BD*(1) C2–C24 result in the stabilization energy of 20.80 and 18.36 kcal mol^{-1}, respectively. Consequently, it can be concluded that the antibonding BD*(1) C2–N3 has higher electron density than that of BD*(1) C2–C24, and hence the rupture of the C2–N3 bond may be easier compared to C2–C24. Nevertheless, we think that the rupture occurs in the bondC2-C24 for the next reason (i) attractive force between C2 and N3 bigger than attractive force between C2 and C24 (ii) the withdrawing effect of O1 and N3 on C2 atom charge (0.611e) and C24 (-0.183e) causes elongation of bond C2-C24 (1.526Å). The same trend and conclusion can be obtained for the same two bonds in $[DOX]^+$ molecule, since the interaction of LP(2) O1 in this molecule with BD*(1) C2–N3 and BD*(1) C2–C24 has stabilization energy of 11.20 and 8.53 kcal mol-1, respectively.

Table 3: Second order perturbation theory analysis of Fock matrix in NBO basis of Cation DOX molecule(selected).

Donor NBO(i)	Acceptor NBO(j)	E^2 (kcal/mol)	ΔE a.u.	F(i,j) a.u.
BD (2) C7 - N8	LP*(1) C9	38.77	0.17	0.120
BD (2) C11 - C12	LP*(1) C9	25.50	0.14	0.088
BD (2) C11 - C12	BD*(2) C20 - N21	13.99	0.25	0.082
BD (2) C16 - C19	BD*(2) C20 - N21	16.00	0.24	0.085
BD (2) C20 - N21	BD*(2) C7 - N 8	20.34	0.28	0.103
BD (2) C26 - C27	BD*(2) C30 - C31	10.35	0.29	0.070
BD (2) C28 - C29	BD*(2) C26 - C27	11.48	0.26	0.070
BD (2) C28 - C29	BD*(2) C30 - C31	11.01	0.26	0.069
BD (2) C30 - C31	BD*(2) C26 - C27	10.85	0.28	0.070
BD (2) C30 - C31	BD*(2) C28 - C29	9.82	0.29	0.068
LP (2) O1	BD*(1) C2 - N3	11.20	0.68	0.111
LP (2) O1	BD*(1) C2 - C24	8.53	0.60	0.092
LP (1) N3	BD*(2) O1 - C2	27.88	0.29	0.114
LP (1) N6	BD*(2) C7 - N8	28.05	0.26	0.115
LP (1) N6	BD*(1) C22 - C23	1.89	0.65	0.047
LP*(1) C9	BD*(2) C7 - N 8	28.37	0.11	0.084
LP*(1) C9	BD*(2) C11 - C12	28.07	0.14	0.093
LP (1) N10	LP*(1) C9	63.49	0.13	0.135

E^2 means energy of Hyperconjugative interactions

$\Delta E = Ej - E_i$ is the energy difference between donor (i) and acceptor (j) NBO orbitals; F = F(i, j) is the Fock matrix element between i and j NBO orbitals

3.2 Proposed fragmentation pathway by MS

Mass spectral fragmentation of DOX ionized drug molecule using EI-MS at 70 and 15 eV are shown in Fig (3.a, b).

The EI spectra of DOX at 70 eV (Fig 3a) consist of a wealthy, competitive and consecutive fragment ions ranging from m/z = 43 up to molecular ion at m/z = 451, in which the signal appeared at m/z = 451 (RI = 20.32 %) is related to the molecular ion $[M]^+$ of general formula $[C_{23}H_{25}N_5O5]^+$. This molecular ion represents 20.32 % of the base peak at m/z = 233 (RI = 100%). The main fragmentation pathways following EI of DOX at 70 eV may be given by the proposed scheme (1).

Pathway (1) refers to the formation of fragment ions of m/ z = 233 (RI = 100 %) and 205 (RI = 28.74 %) of the formulae $[C_{11}H_{12}N_4O_2]^+$ and $[C_{10}H_{10}N_3O_2]^+$ obtained as a result of rupture of bonds C22-C33 and N6-C5 bonds respectively.

Rupturing of C2-C24 bond leads to pathway (2 and 3). Pathway (2) refers to the formation of fragment ions of m/z = 135 (RI = 8.580 %) of the formulae $[C_8H_7O_2]^+$ and pathway (3) refers to the formation of fragment ion m/z = 316 (RI = 24.56 %) of the formulae $[C_{15}H_{18}N_5O_3]^+$ and then fragment ion m/z =288 (RI =6.500%) of the formulae $[C_{14}H_{18}N_5O_2]^+$ as a result of rupture of bond N1-C21. Measuring mass spectra of DOX by EI at lower power of 15 eV (Fig 3.b) refers to change in nature of the previously fragment ions obtain using EI at 70 eV. At 15 eV the base peak becomes m/z = 451 (RI = 100%) of $[M]^+$ of the drug main molecule, and RI of the fragment ion of m/z = 233 decreases (RI = 10.43 %). This means that; lowering the energy of the power source increases RI of the drug main molecular ion and makes lot of fragment ions, obtain at 70 eV, of low RI and / or completely disappear.

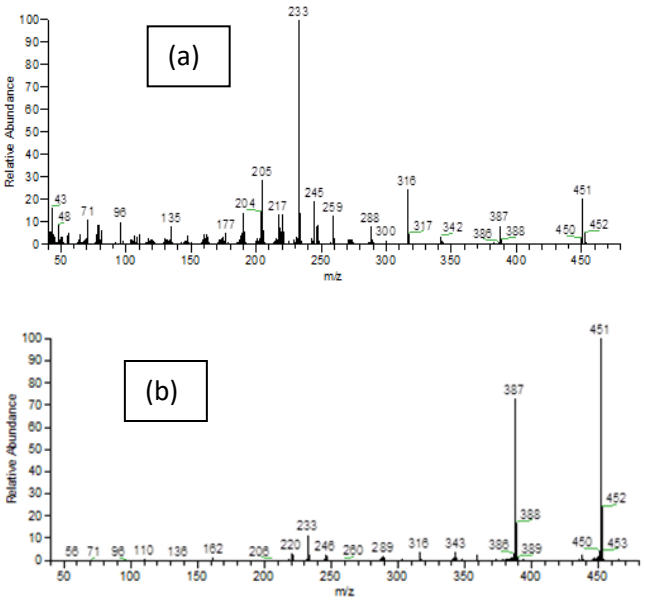

Fig. 3: Mass spectrum of doxazosin EI at (a)70 and (b)15eV

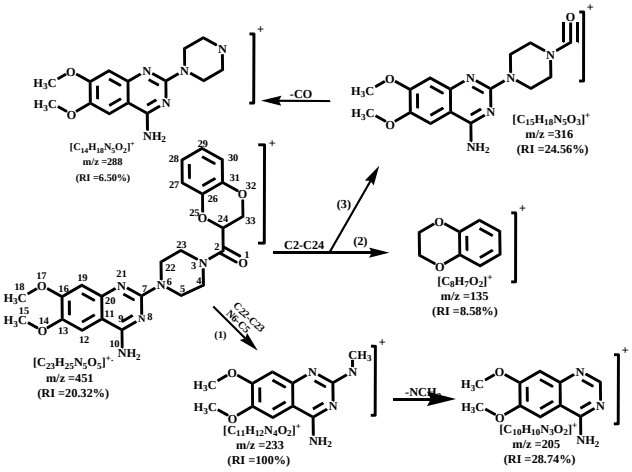

Scheme (1) shows three competitive and consecutive fragmentation pathways.

3.3 Proposed thermal decomposition of DOX drug

The thermal analyses data of DOX are shown in Fig (4.a, b).

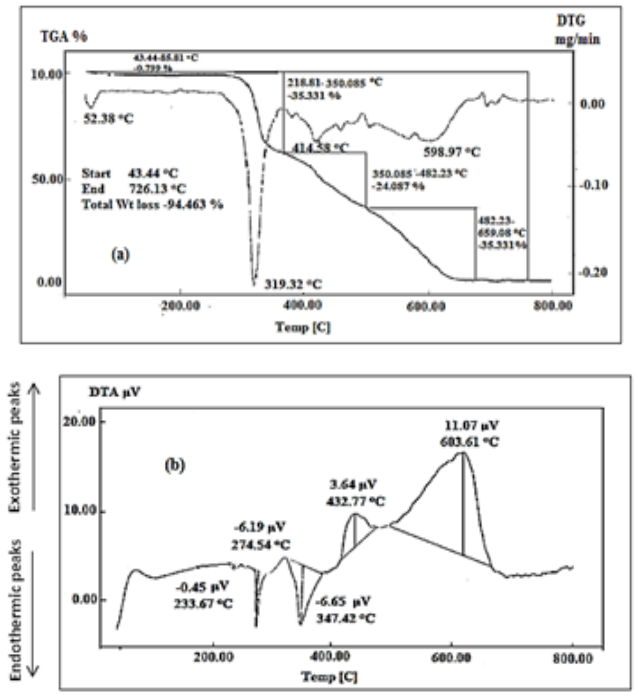

Fig (4): Thermal analyses of standard DOX drug: (a) TGA/DTG (b) DTA

From TGA and DTG thermograms (Fig 4a), it is clear that DOX decomposed in three main steps within temperature range 43.44-659.1 °C with practical total weight loss of 94.749%. The first step occurs at (218.8-350.3 °C) and exactly at 319.3 °C (from DTG curve); which may be related to the loss of $C_{11}H_{11}NO_3$ radical as a result of rupture of two weak bonds C22-C23 and C4-C5 (Pract. % = 35.331 %, Calcd. % = 37.47 %). This weight loss is confirmed by the appearance of endothermic peak in DTA (Fig 4b) at temperature 347.42 °C.

The second step at (350.3–482.2 °C) and exactly at 414.6 °C (from DTG curve); this may be attributed to the loss of $C_2H_7N.CH_3O_3S$ as a result of rupture of the weak bond N4-C7 (Pract. % = 24.09 % and Calcd. % = 25.57 %). It appears as exothermic peak in DTA at 432.8 °C; which may refers to chemical rearrangement and/or chemical recombination of the fragments. The third step at (482.2-659.1 °C) and exactly at 598.9 °C (from DTG curve); this may be attributed to the loss of $C_{10}H_{10}N_2O_2$ molecule (Pract. % = 35.33 % and Calcd. % = 34.68 %) as a result of rupture of the weak bond C9-N10. It appears as strong exothermic peak in DTA at 603.6 °C; which may refers to chemical rearrangement and/or chemical recombination of the fragments to give the final chemical formula.

A small endothermic peak appears in DTA at 233.7 °C; this may be due to phase transition of DOX from polymorphic form to another one melts at 274.54°C (the second endothermic peak). This melting point represented as a sharp endothermic peak [37].

Therefore, these thermal decomposition endothermic peaks and chemical exothermic rearrangements of thermal decomposition of DOX may be represented by the scheme (2). A comparison between TA (scheme 2) and MS (scheme 1) refers to the coincidence between the TA description and MS pathway 1.

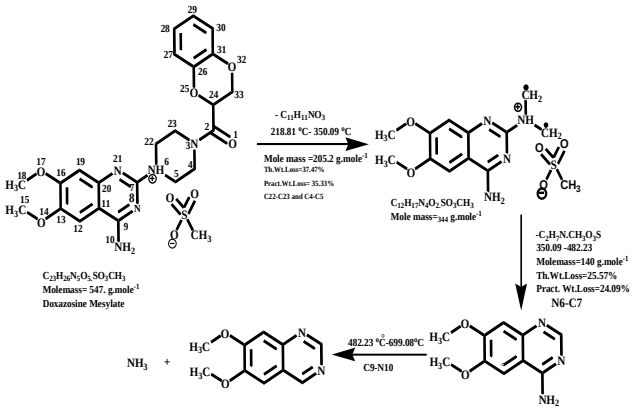

Scheme (2): Proposed thermal decomposition of DOX drug in neutral form.

3.4 Correlation between TA, MS fragmentation of Doxazosin compound in comparison with the MOC data

In this investigation we search for prediction and discern features of initial bond ruptures occurring during the practical TA and MS fragmentation of doxazosin. The density functional theory (DFT) calculations and natural bond orbital (NBO) analysis can provide additional data which can be used for interpretation of experimental results using numbering system (Fig. 1). The initial location of charges on atoms (Table 1) of neutral molecules is used in TA fragmentation interpretation and ionic forms in MS interpretation which is of particular importance in driving fragmentation of the parent drug [38].

In TA, some bonds are thermally unstable in neutral form (Fig. 2a); and consequently decomposed in TG as consecutive pathway. These bonds are C22–C23 (1.534)\C4–C5 (1.532)\C7–N6 (1.337), which ordered from the weakest to the strongest bond as estimate from DFT and NBO calculations of neutral Doxazosin as represented in Scheme 2. In EI, MS at 70 eV high powers energy leads to more bond ruptures including those ruptured in TA. These bonds are C22–C23 (1.534))\C4–C5 (1.532) \ C2–C24 (1.526\ C5–N6(1.466)\C7–N6(1.377), respectively, which ordered from the weakest to the strongest as estimate from DFT and NBO calculations of the cation of Doxazosin (Table 1). This comparison shows the agreement to some extent between TA and EI Mass in the proposed

fragmentation pathways. Consequently, the effect of such fragmentation on the drug behavior in human body can be expected and also its metabolites can easily be identified. The obtained thermal fragments and mass fragment ions obtained in vitro system are found to be very similar to metabolites obtained in vivo systems [39]. This conclusion reveals the importance of TA and MS vitro systems before going to search for metabolites in vivo system.

4 Conclusions

Doxazosin is an alpha1-adrenoceptor blocker with actions and uses similar to those of prazosin, but a longer duration of action. It is used in the management of hypertension and in benign prostatic hyperplasia to relieve symptoms of urinary obstruction**.** Due to this importance, in the present study, MS and TA were used to propose the fragmentation decomposition pathways of doxazosin and confirmed by molecular orbital (MO) calculations, using density functional theory (DFT) and natural bond orbital (NBO) analysis on the neutral and the positively charged species of the drug. The mass spectra and TA fragmentation pathways were proposed and compared to each other to select the most suitable scheme representing the correct fragmentation pathway of the drug in both techniques. This selection helps understanding of metabolism of the drug in vivo system. Therefore, the successful comparison between MS and TA helps in selection the proper pathway representing the fragmentation of this drug. This comparison successfully confirmed by MO calculation.

References

[1] Barker, James. *Mass Spectrometry, 2nd, John Wiley & Sons: Chichester, England,1999.*

[2] Barbas R, Prohens R, Puigjaner C. *J Therm Anal Calorim.* **2007**,89. 687.

[3] Pentak D, Sułkowski WW, Sułkowska A.. *J Therm Anal Calorim.* **2008**, 93, 471.

[4] Picker-Freyer KM. *J Therm Anal Calorim*. **2007**, 89, 745

[5] Santos AFO, Basílio ID Jr, de Souza FS, Medeiros AFD, Pinto MF, de Santana DP, et al. *J Therm Anal Calorim.* **2008**, 93, 361.

[6] Michalik K, Drzazga Z, Michnik A. *J Therm Anal Calorim.* **2008,** 93, 521.

[7] Pourmortazavi SM, Hajimirsadeghi SS, Hosseini SG. *J Therm Anal Calorim*. **2006**, 84, 557.

[8] Lever SD, Papadaki M. Study of condition-dependent decomposition reactions: *J Hazard Mater*. **2004**, 115, 91.

[9] Pourmortazavi SM, Hosseini SG, Hajimirsadeghi SS, Fareghi Alamdari R. *Combust Sci Tech*. **2008**, 180, 2093.

[10] Hosseini SG, Pourmortazavi SM, Hajimirsadeghi SS. *Combust Flame*. **2005**, 141, 322

[11] Fahmey, M.A.; Zayed, M.A.; Keshk, Y.H.; *Thermochim. Acta.*, **2001**, 366, 183.

[12] A.Somogyi, A.Gomory, K.Vekey, J.Tamas, *Org.Mass Spectrom*., **1991**, 26, 936

[13] Fahmey, M.A.; Zayed, M.A.; *J. Therm. Anal. Calorim.*, **2002**, 67, 163.

[14] Fulton, B., Wagstaff, A. J., Sorkin, E. M., *Drugs*, **1995**, 49, 295.

[15] Kirby, R., Andersson, K. E., Lepor, H., Steers, W. D., *Prostate Cancer Prostatic Dis.*, **2000**, 3, 76 – 83.

[16] Akduman, B., Crawford, E. D., *Urology*, **2001**, 58, 49 – 54.

[17] Goldsmith, D. R., Plosker, G. L., *Drugs*, **2005**, 65, 2038 – 2047.

[18] Lepor, H., Rev. Urol., 2006, 8, S3 – S9.

[19] Fulton, B., Wagstaff, A. J., Sorkin E. M., *Drugs*, **1995**, 49, 295 – 320.

[20] Bakshi M., Ojha T., Singh S., *J. Pharm. Biomed. Anal.* **2004**, 34, 19.

[21] Kwon Y.H., Gwak H.S., Yoon S.J., Chun I.K., *Drug Dev Ind. Pharm*. **2007**, 33, 824.

[22] Sripalakit P., Nermhom P., Saraphanchotiwitthaya A., *Biomed. Chromatogr*. **2006**, 20, 729.

[23] Kim Y.J., Lee Y., Kang M.J., Huh J.S., Yoon M., Lee J., Choi Y.W., *Biomed. Chromatogr*. **2006**, 20, 1172.

[24] P. Sripalakit, P. Nermhom, A. Saraphanchotiwitthaya, *J. Chromatogr. Sci*. **2005**, 43, 63.

[25] Jackman G.P., Colagrande F., Louis W.J., *J. Chromatogr.* **1991**, 566, 234.

[26]. Fouda H.G, Twomey T.M., Schneider R.P., *J. Chromatogr. Sci.* **1988**, 26, 570.

[27] Cowlishaw M.G., Sharman J. R. , *J. Chromatogr*. **1985**, 344, 403.

[28] Erceg M., Cindric M., Pozaic F.V., Vertzoni M., Cetina-Cizmek B., Reppas C., *J. Chromatogr. Sci.* **2010**, 48, 114.

[29] Ma N., LiuV, Li H., Chen B., Zhu Y., Liu X., Wang F., D. Xiang, B. Zhang, *J. Pharm. Biomed. Anal.* **2007**, 43, 1049.

[30] H.Y. Ji, E.J. Park, K.C. Lee, H.S. Lee, *J. Sep. Sci.* **2008**, 31, 1628.

[31] S. Fdez de Betono, A. Arranz Garcia, J.F. Arranz Valentin, *J. Pharm. Biomed. Anal*. **1999**, 20, 621.

[32] Arranz A., de Betono S. F., Moreda J.M., Cid A., Arranz J.F., *Analyst.* **1997**, 122 849.

[33] Becke A.D., *J. Chem. Phys*. **1993**, 98,5648–5682.

[34] Lee C., Yang W., Parr R.G., *Phys. Rev. B* **1998**, 37, 785–789.

[35] Frisch MJ, Trucks GW, Schlegel HB, Scuseria GE, Robb MA, Cheeseman JR, Scalmani G, Barone V, Mennucci B, Petersson GA, Nakatsuji H, Caricato M, Li X, Hratchian HP, Izmaylov AF, Bloino J, Zheng G, Sonnenberg JL, Hada M, Ehara M, Toyota K, Fukuda R, Hasegawa J, Ishida M, Nakajima T, Honda Y, Kitao O, Nakai H, Vreven T, Montgomery JA Jr, Peralta JE, Ogliaro F, Bearpark M, Heyd JJ, Brothers E, Kudin KN, Staroverov VN, Keith T, Kobayashi R, Normand J, Raghavachari K, Rendell A, Burant

JC, Iyengar SS, Tomasi J, Cossi M, Rega N, Millam JM, Klene M, Knox JE, Cross JB, Bakken V, Adamo C, Jaramillo J, Gomperts R, Stratmann RE, Yazyev O, Austin AJ, Cammi R, Pomelli C, Ochterski JW, Martin RL, Morokuma K, Zakrzewski VG, Voth GA, Salvador P, Dannenberg JJ, Dapprich S, Daniels AD, Farkas O, Foresman JB, Ortiz JV, Cioslowski J, Fox DJ. *Gaussian 09. Revision C01. Wallingford: Gaussian Inc.;* **2010**.

[36] Glendening ED, Badenhoop JK, Reed AE, Carpenter JE, Weinhold F. NBO. Version 3.1. Madison: *Theoretical Chemistry Institute, University of Wisconsin;* **1995**.

[37] Grčman M., Vrečer F., Meden A.; *J Therm Anal Cal,* **2002**, 68,373-387.

[38] Zayed EM, Zayed MA, Hindy AMM. *J Therm Anal Calorim.;* **2014**, 116, 391–400.

[39] Ey O, Base SK, Kwon JW, You M, Lee DC III, Lee MG. Br; *J Pharmacol*.; **2007**,15,1 24–34.